Published in final edited form as:
Acc Chem Res. 2013 December 17; 46(12): . doi:10.1021/ar400061d.

Ion channel models based on self-assembling cyclic peptide nanotubes

Javier Montenegro[†], **M. Reza Ghadiri**[‡], and **Juan R. Granja**[†]

[†]Departamento de Química Orgánica, Centro Singular de Investigación en Química Biológica y Materials Moleculares (CIQUS), Universidad de Santiago de Compostela (USC), Campus Vida, 15782 Santiago de Compostela, Spain.

[‡]Departments of Chemistry and Molecular Biology, and the Skaggs Institute for Chemical Biology, The Scripps Research Institute, 10550 North Torrey Pines Road, La Jolla, California 92037.

CONSPECTUS

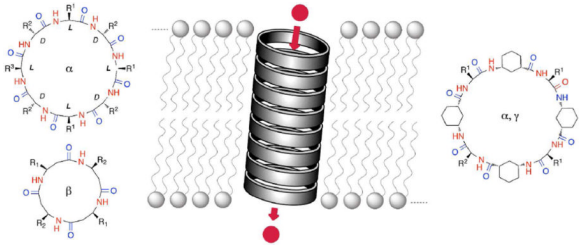

Compartmentalization and isolation from external media facilitates the sophisticated functionality and connectivity of all the different biological processes accomplished by living entities. The lipid bilayer membranes are the dynamic structural motifs selected by Nature to individualize cells and keep ions, proteins, biopolymers and metabolites confined in the appropriate location. However, cellular interaction with the exterior and the regulation of its internal environment requires the assistance of minimal energy short cuts for the transport of molecules across membranes. Ion channels and pores stand out from all other possible transport mechanisms due to their high selectivity and efficiency in discriminating and transporting ions or molecules across membrane barriers. Nevertheless, the complexity of these smart "*membrane holes*" has been a significant driving force to develop artificial structures with comparable performance to the natural systems. The emergence of the broad range of supramolecular interactions as efficient tools for the rational design and preparation of stable 3D superstructures has boosted the possibilities and stimulated the creativity of chemists to design synthetic mimics of natural active macromolecules and even to develop artificial functions and properties. In this account we highlight results from our laboratories on the construction of artificial ion channel models that exploit the self-assembling of flat cyclic peptides into supramolecular nanotubes. The straightforward synthesis of the cyclic peptide monomers and the complete control over the internal diameter and external surface properties of the resulting hollow tubular suprastructure make CPs the optimal candidates for the fabrication of ion channels. Ion channel activities and selective transport of small molecules are examples of the huge potential of cyclic peptide nanotubes for the construction of functional transmembrane ion channels or pores. Our experience to date suggests that the topological control over cyclic peptide assembly together with the lumen functionalization should be the next steps to achieve conceptual devices with better performance and selectivity.

Correspondence to: M. Reza Ghadiri; Juan R. Granja.

Supporting Information
Tables 1 and 2 are included. This information is available free of charge via the Internet at http://pubs.acs.org/.

1. Introduction

The selective and efficient transport of ions, metabolites and biopolymers across biological membranes is essential for cell vitality.[1] The transport of ions and molecules into and out of cells can occur by different mechanisms, such as ion channels, pores, carriers, passive diffusion and endo-/exo-cytosis. Of all the available transport processes, ion channels are exquisitely regulated for the modulation of ion flow and selectivity across lipid bilayers.[2] Natural ion channels and pores regulate numerous biological functions, such as ion flow, signal transduction and molecular transport. The functional ion channel or pore can be considered as a “hole” in the phospholipid membrane that minimizes the inherent repulsion between water-soluble molecules and the hydrophobic lipid environment.[3] Evolution has produced highly adapted and complex functional structures for ion[4] or water[5] transport across membranes. This impressive degree of complexity is perhaps the main challenge that chemists have encountered in designing synthetic ion channels[6–8] or transporters.[9] Nevertheless, the fundamental features used by Nature to achieve this formidable task, such as size exclusion, charge repulsion, ion hopping, hydrogen bonding, ion pairing, hydrophobic or hydrophilic interactions, afford a vast resource to inspire the design and construction of artificial ion channels and carriers.[6–9]

The ability to coax molecules into tubular ensembles[10] provides an important structural requirement in the design of functional ion channels or pores.[6–8] Pore-forming molecules can benefit from partial solubility in water, but they need to have good partition coefficients and assembly properties in the lipid bilayer, be long enough to span the membrane, and be reasonably stable to generate the requisite open state. The optimal candidate would be available with a controlled shape, size and chemical functionalization and would be prepared by a facile synthetic methodology. In our laboratories we have tackled the construction of artificial ion channels and pores by using nanotubes that consist of stacks of self-assembling cyclic peptide (CP) monomers.[11] In the last few years we have demonstrated the usefulness and versatility of these scaffolds to accomplish a wide variety of transport duties.

2. Cyclic $_{D,L}$-α-peptides

In linear α-peptides, the alternation of amino acid chirality (*L*, $_{D,L,D}$, etc.) inverts the backbone dihedral angles (ϕ_L, $\Psi_L = \phi_D, -\Psi_D$)to afford helical pleated structures with minimized side-chain interactions and β-type hydrogen bonding.[10] The resulting β-helical motifs with hydrophilic interiors are present in pore-forming natural peptides such as gramicidin A.[12] Despite the possible modulation of their supramolecular assembly, the high entropy of linear peptides would prevent precise control and predictability of the desired functional structure. Consequently, less promiscuous but also adaptable frameworks are preferable; a situation that brings us to the realm of cyclic *D*,*L*-α-peptides (*D*,*L*-α-CPs).

Although theoretically envisaged in 1974,[13] the formation of hollow tubular structures by the stacking of $_{D,L}$-α-CPs was not demonstrated until 1993.[14] The compound cyclo-[(D-Ala-L-Glu-D-Ala-L-Gln-)$_2$] (**CP1**) was chosen due to its pH-dependent solubility in water, with the monomers being water soluble under basic conditions and self-assembled upon acidification (Fig. 1a). The anticipated supramolecular structure of self-assembled cyclic peptide nanotubes (SCPNs) was unambiguously confirmed by electron microscopy, electron diffraction, FT-IR spectroscopy and crystal structure modeling of the resulting microcrystals.[14] The self-association pattern of cyclic peptides through an antiparallel β-sheet hydrogen-bonding network[15,16] is derived from the flat conformation of the CP rings. In this conformation the amino acid (Aa) side chains diverge outwards from the nanotube. In the resulting tubular ensemble, the nanotube diameter and chemical surface properties can

be easily adjusted by simply changing the ring size and sequence of CPs. Importantly, the chemical synthesis of CPs can be easily achieved by the standard solid-phase synthetic methodology.[17]

The hydrophobic tryptophan and leucine decoration of cyclo-[D-Leu- L-Gln-(D-Leu-L-Trp-)$_3$] (**CP2a**) proved to be ideal for the integration of the nanotube in the non-polar environment of the membrane. Besides, the enthalpy-driven self-assembly of the rings is intensified by hydrogen-bond formation in this medium.[18] A discrete nanotube made up of eight D,L-α-CPs is represented in Fig. 2b. This nanotube is long enough to span a lipid bilayer and furnish the desired transmembrane functional structure.[15]

The incorporation of the peptide into the membrane of large unilamellar vesicles (LUVs) was established by UV absorption and fluorescence spectroscopy. The expected putative hydrogen-bonded tubular structure was confirmed by FT-IR, which showed bands that correlated well with hydrogen-bonded amide I and amide II bands (~1620 cm^{-1}, ~1530 cm^{-1}) and an N–H stretching band (~3300 cm^{-1}). An insight into the orientation of the peptide nanotubes in lipid bilayers came from a study involving different and complementary infrared techniques. The parallel polarized grazing angle IR spectrum of a gold-supported multilayer of **CP2a** mixed with DMPC (1,2-dimyristoyl-*sn*-glycero-3-phosphocholine) revealed high values for the ratio between amide I (⊥) and amide II bands. According to the infrared selection rules, the prevalence of the amide I (⊥) band qualitatively demonstrated the alignment of the nanotube along the surface (parallel to the lipid aliphatic chains). Furthermore, a careful analysis of the polarized ATR-IR amide I (⊥) dichroic ratio indicated a nanotube tilt angle of 7 ± 1° relative to the membrane plane (Fig. 2b). Interestingly, such an orientation is sequence-dependent and, in the case of amphiphilic CPs, the orientation, as expected, was found to be parallel to the membrane layer, *vide infra* (Fig. 4d).

The proton transport ability of the channel was addressed by using 5-(6)-carboxyfluorescein (CF) loaded vesicles (LUVs⊃CF) with an induced pH gradient (pH_{out} = 5.5; pH_{in} = 6.5). Addition of the channel-forming peptide to the liposomes immediately triggered the influx of protons from the extra-vesicular medium, thereby decreasing the fluorescence of the internal pH-sensitive dye. Control experiments with the more hydrophilic cyclo-[(D-Leu-L-Gln-)4] (**CP3**) (inhibited partition) and the dimeric cyclo-[(D- ^{Me}*N*-Ala-L-Phe-)$_4$] (**CP4**, Fig. 1b)[15] confirmed transport activity through the presumed trans-membrane suprastructure. Possible leakage and/or carrier transport mechanisms for **CP2a** were ruled out on the basis of control experiments involving LUVs⊃CF at self-quenched concentrations. It is important to remark that these results did not provide any information about ion-transport rates, which are on a much faster time scale, but did confirm the peptide diffusion into the lipid bilayer and nanotube formation, both of which represent the rate-limiting step. The definitive evidence for channel activity in **CP2a** came from conductance experiments in planar bilayer membranes (BLMs).[2,7] The addition of **CP2a** (1 nM final concentration) into the sub-phase volume of the micro patch-clamp device spontaneously gave rise to stochastic single channel events (Fig. 2c). The observed open-closed transitions were initially assigned to assembly-disassembly processes and/or nanotube collapse due to the structural flexibility of the CP ring (Fig. 3b). The recorded conductance values for equimolar concentrations (500 mM) of NaCl and KCl were 55 and 65 picosiemens (pS), respectively. The calculated ion-channel transport rate was three times faster than for gramicidin A under similar conditions.[20]

In general, SCPNs proved to be efficient transporters of alkali metal (group 1) (**CP2b**, Table 1 of SI)[21,23] for which the maximum conductance data (g_{max}) indicated that transport of cations followed the lyotropic series. Apparently, nanotube channels transport only one ion

at a time based on the fact that conductance values did not change significantly at high electrolyte concentrations and that the data fitted a first-order Michaelis–Menten equation. A significant decrease in the conductance occurs only at high CsCl concentrations, indicating that, under these conditions, two cations might be located in the channel at the same time.[1] Cation over anion selectivity was determined by measuring the reversal potentials (E_r) when the two chambers contained different salt concentrations (KCl or NaCl)., E_r is the potential that must be applied to counteract the chemical gradient that is established across the lipid bilayer. This parameter can be related to the permeabilities of the different ions in solution and their activities by the Goldman–Hodgkin–Katz equation.[1] In all cases studied, reversal potentials (P_{K+}/P_{Cl-} >200) confirmed the strong cation selectivity.[21] In addition, channel conductance experiments also showed that divalent cations such as calcium were not transported through this family of ion channels.

In general, all recordings showed different conductance levels and this suggests the presence of transporting nanotubes composed of different numbers of CP subunits (Fig. 3).[21] Thus, on examining the conductance behavior of **CP2b** over a long time period (100 mM KCl and 100 mV, t > 50 s), four independent conductance levels (24.8, 20.7, 18.3 and 14.1 pS) could be distinguished. In a simplified situation where diffusion coefficients and effective areas remain unchanged for the possible ensembles, the correlation of the conductance with the channel length could be estimated with the Nernst–Planck electrodiffusion equation (Eq. 1), where *z* is the charge of the ion, F and R are the Faraday and gas constants, respectively, D_+ and D_- are the corresponding diffusion coefficients for the cation and anion, *c* is the concentration of the electrolyte used and *A* is the effective channel cross section.[22]

$$g = \left(\frac{z^2F^2}{RT}\right) \bullet \left(\frac{(D_+ + D_-)cA}{l}\right) \quad \text{(Eq. 1)}$$

In the membrane, the length of the potential membrane-partitioned ensembles is restricted to multiples of the inter-ring distance (4.85 Å)[16] due to the structural features of the SCPNs. Hence, using Eq. 1, the calculated conductance ratios for channels composed of 5, 6, 7 and 8 CPs (24 to 39 Å in length) were found to be 1.00, 0.83, 0.71 and 0.62, respectively. These estimated conductance ratios are in good agreement with the experimentally obtained values of 1.00, 0.83, 0.74 and 0.57, thus supporting the model of dynamic transporting nanotubes in which the number of CP subunits is inversely proportional to the channel conductance.[21] The channels that consist of five stacked subunits of CPs (24 Å) were the most commonly observed species and this is consistent with the minimum thickness of the hydrophobic part of the lipid bilayer.

Further investigation of the conducting properties of a series of CPs with different ring sizes (CPs with six, eight, ten and twelve residues) and different Aa compositions showed that the channel dwell opening time (τ) was inversely proportional to the diameter and the hydrophilicity of the CPs assembled in the functional nanotube (Table 2, SI).[21,23] These observations could be explained by the lower conformational freedom of the smaller cyclic peptides and the hindered intersubunit interaction and/or lower affinity for the membrane environment in the case of the more polar CPs.[23]

Validation of ion channel activities, together with the X-ray diffraction analysis results on the water-filled dimeric structure **D4** (Fig. 1c,d),[16] unequivocally established the presence of an aqueous transmembrane channel for cyclic peptide nanotubes. The water organization and self-diffusion inside SCPN channels were investigated for **CP1** by means of molecular dynamics.[24] The computer simulation showed a water-filled and stable supramolecular nanotube during the entire calculation time (760 ps). The model showed a tendency for the

water molecules to be organized in alternate layers with one water molecule in the region near the peptide plane and two water molecules in the inter-ring regions and up to 27 water molecules for the original canonical state. However, the number of water molecules increased gradually during the simulation time. This deviation from the canonical state led to defects in the inner-water string, a situation that suggests a possible hopping mechanism for the water diffusion.

Having achieved the first complete characterization of SCPNs as functional ion channels, the second main aim was to exploit this tubular assembly for the selective membrane transport of polar molecules. Molecular modeling suggested that a pore diameter greater than 9 Å could accommodate a glucose molecule within the nanotube lumen. Simple elongation of **CP2a** by the addition of two extra Aas would yield decapeptide cyclo-[D-Leu-L-Gln-(D-Leu-L-Trp-)$_4$] (**CP5**) with an internal diameter of 10 Å. As mentioned before, **CP5** also transported alkali metal ions but the mean opening times were shorter than those for **CP2a**, probably due to the increased conformational freedom of the decapeptide. Non-symmetrical NaCl experiments again indicated significant selectivity for cations over anions.[20] **CP5** was subsequently tested for molecular transport using glucose-entrapped LUVs.[25] Glucose efflux was measured by UV detection of the NADH (λ_{abs} = 340 nm) produced in a glucose-triggered enzymatic coupled assay (Fig. 2d). Addition of **CP5** to isotonic suspensions of the aforementioned LUVs⊃Glucose immediately triggered glucose transport with first-order kinetics. This transport increased gradually on augmenting the peptide concentration. The absence of saturation for the observed linear relation between transport rate and glucose concentration and the negative leakage control experiments are in good agreement with a pore-forming mechanism for the nanotube-assisted transport. On the other hand, the smaller peptide **CP2a** did not show any glucose transport activity under similar conditions, a finding that supports size-selectivity through a pore-mediated transport mechanism.

Size-selective transport was also achieved for small charged molecules like amino acids.[26] Once again, molecular modeling suggested that glutamic acid size-selective transport could be achieved through decapeptide **CP5**. An enzymatic couple assay of sodium glutamate entrapped liposomes was used to evaluate the glutamate transport properties. The addition of either gramicidin A (negative control), **CP2a** or **CP5** to the LUVs⊃NaGlu assay initiated the concentration-dependent glutamate efflux exclusively in the case of **CP5**. Glutamate transport was also measured in planar BLMs by replacing the *trans* buffer for an equimolar solution of NaGlu. In these conditions, the bi-ionic potential of **CP2a** was almost identical to that of gramicidin A, thus confirming the failure of **CP2a** to transport glutamate. On the other hand, **CP5** presented a higher reversal potential (Fig. 2e) as a consequence of the glutamate transport.[26] At 1.0 mM CP concentration, the estimated rate of transport of Glu was $2.7 \cdot 10^4$ molecules per second.

The validation and quantification of ion and molecular transport through SCPNs encouraged the preparation of more complex functional structures such as heteromeric nanotubes with modified transport capabilities. This approach was designed on the basis that ionic amphiphilic CPs, such as **CP6-9** (Fig. 4), would remain at the lipid-water interface and interact, as a molecular cap, with the transmembrane nanotubular assembly of the hydrophobic **CP2b** (Fig. 4b).[27] Such peptides could modify nanotube transport properties through local electrostatic perturbations brought about by the charged groups. With this aim in mind, CPs bearing ammonium (**CP8**), guanindinium (**CP6**) and carboxylate (**CP7, CP9**) moieties were prepared for a location-controlled assembly with the transporting **SCPN2b**. Planar BLMs experiments were carried out and it was found that the maximal conductance of **CP2**b either decreased or increased depending on the addition (on one or both sides of the buffers) of cationic (**CP6, CP8**) or anionic (**CP7, CP9**) charged peptides. This non-ohmic

current rectification was insensitive to changes in the membrane composition, thus ruling out the occurrence of non-specific interactions of hydrophilic CPs with the lipidic head groups.

The possibility of exploiting the selective transport capabilities of SCPNs for the fabrication of functional devices was exemplified by the construction of diffusion-limited size-selective ion sensors.[28] The designed architecture consisted of discrete nanotubes of **CP2b** embedded inside organosulfur self-assembled monolayers (SAMs) deposited on gold surfaces (Fig. 4c). In order to maximize the perpendicular (to the gold surface) arrangement of the nanotubes, the hydrophobic **CP2b** was incorporated into SAMs using either a stepwise or a co-adsorption protocol. Inspection of the grazing angle FTIR absorption spectra (amide I and amide II bands) indicated that the best results were obtained by initial deposition of alkanethiols followed by immersion in CP solutions (stepwise method). Cyclic voltammetry experiments showed activity only for the small redox couple $[Fe(CN)_6]^{3-}/[Ru(NH_3)_6]^{3+}$ whereas the large couple $[Mo(CN)_6]^{3-}$ /$[Ru(NH_3)_6]^{3+}$ (too large to enter the pore) was inactive. These observations ruled out the occurrence of any redox activity due to monolayer defects and validated SCPN devices as useful size selective ion sensors.

This CPs were also exploited to expand the previously discovered ability of cyclodextrins to alter the properties of the pore-forming protein staphylococcal α-hemolysin (α-HL).[29] The hydrophilic octapeptides **CP6-9** were deposited into the lumen of α-HL by applying an external potential.[30] The CPs affinity towards α-HL was sensitive to the charge of the peptide and the applied potential, suggesting that the CP binding was taking place inside the channel of the protein. The protein conductance was reduced (~50–90%) after the peptide binding and the intrinsic anion selectivity of α-HL was augmented for positively charged peptides and inverted to weak cation selectivity for the negatively charge CPs. These experimental observations confirmed the applicability of CPs for the constriction and rectification of pore-forming proteins; nevertheless, the final mechanism for the ion flow remains elusive due to the potential conformational promiscuity of CPs.

Promising vesicular and molecular transport results for certain CPs encouraged research effort aimed at the application of this particular tubular motif as antibacterial therapeutic agents.[31] The octapeptide **CP10**, cyclo-[D-Lys-L-Gln-D-Arg-L-Trp-(D-Leu-L-Trp-)$_2$], displayed a potent *in vitro* activity against Gram-positive and Gram-negative bacteria. The straightforward synthetic access to CPs with different ring sizes and amino acid compositions allowed the rapid preparation of a series of amphiphilic CPs. The study of these systems clarified the role of CP hydrophilicity in the biological activity and membrane selectivity. The estimated tilt angle for this type of CP in oriented DMPC lipid multi-bilayers (70 ± 5°), i.e. almost parallel to the membrane surface, suggested a ‘carpet-like’ mode of action for the membrane-disrupting antibacterial activity (Fig. 4d). Recently, it was found that specific glycosylation of amphiphilic CPs significantly reduced the cell toxicity in mammalian cells while maintaining the bactericidal activities against multidrug-resistant Gram-positive bacteria.[32]

2. Cyclic β-peptides

In a similar way to the D,L-α-CPs counterparts, the side chains of homochiral β^3-CPs radiate equatorially from the peptide ring plane; however, the additional carbon of β^3-Aa residues give rise to an opposite unidirectional orientation of amide and carbonyl moieties along the nanotube longitudinal axis (Fig. 5). This arrangement generates a net macrodipole moment reminiscent of an α-helix and this could influence the nanotube conductance through effects such as voltage gating and current rectification.[33] In an effort to prove this concept, the ion transport properties of cyclic β-peptides were also studied.

The predicted internal diameter of tetrameric β^3-CPs in a flat ring C_4 conformation (2.6–2.7 Å) would allow the formation of inner channel water strings in the membrane tubular superstructure. Therefore, hydrophobic β^3-CPs, **CP11, CP12** and **CP13**, equipped with tryptophan and/or leucine residues, were synthesized to screen for transport activity (Fig. 5).[34] Inspection of the IR absorbance spectra of **CP11** and **CP12** in DMPC bilayers clearly showed the characteristic hydrogen-bonded nanotube stretching bands. The pH gradient collapse observed in the previously described LUVs⊃CF assay confirmed proton transport for the cyclic peptide fully made of β^3 -triptophane residues (**CP11**), weak activity for **CP12** and no activity for **CP13** due to lack of solubility. The formation of discrete ion channels by compounds **CP11** and **CP12** was conclusively established by conductance measurements in planar BLMs. In 500 mM KCl **CP11** exhibits a conductance of 56 pS and this represents a transport rate of $1.9 \cdot 10^7$ ions per second. Once again, multiple conductance levels and channel gating were present and these were assigned to variations in the number of CP subunits, assembly-disassembly processes and/or ring flexibility. Unfortunately, current rectification behavior of ion channels formed by β-peptides has not been established to date. It is feasible that more robust and rigid tubular structures might be more suitable to apply the macrodipole moments of these structures in the construction of voltage gated ion channels.

3. Cyclic α,γ-peptides

The structural features of the previously described $_{D,L}$-α-CP and β^3 -CP flat-shaped rings inherently inhibited any further chemical modification of the inner cavities in the corresponding nanotubes. The key design feature to overcome this drawback, while maintaining the same self-assembly driven principles of SCPNs, emerged from CPs bearing *cis-3*-aminocycloalkanecarboxylic acid (γ-Aca) residues combined with α-Aas of appropriate chirality, such as α,γ-CP, 3 α,γ-CP or even γ-CP (**CP14**a–c, Fig. 6a). The combination of α- and γ-Aas produced flat rings with non-equivalent faces that had different hydrogen-bonding patterns such as the γ,γ- and the α,α-interactions for the α,γ-CPs (Fig. 6b). As depicted by the X-ray structure of dimeric cyclo-[($_D$-Phe-(1 *R*,3*S*)-γ-^{Me}*N*-Ach-)3] (**CP14c**, R = Bn), the β-methylene moiety of each cyclohexanecarboxylic acid (γ-Ach) was projected into the lumen, thus creating a partial hydrophobic cavity (Fig. 6c). Modifications and possible applications of several γ-Aca scaffolds have been intensively explored and provided a rich variety of tubular structures and nanomaterials.[36]

Molecular modeling of nanotubes (**CP14a**, 6 stacks) in three different solvents (H_2O, MeOH and $CHCl_3$) showed that the nanotube assembly was stable and well preserved throughout the simulation time, being clearly more sensitive to the competition for hydrogen-bonds from the water environment.[37] Methanol was by far the worst guest for this supramolecular structure. Indeed, methanol molecules were not accommodated at all within the nanotube cavity while methanol-filled nanotubes were very unstable. Chloroform diffusion inside the channel was slow but, once internalized, the nanotube was not disturbed for the remaining time, suggesting that α,γ-SCPN might function as a stable container for similar molecules. Despite the partial hydrophobicity of the interior of the nanotube, a wire of 13 to 16 water molecules was immediately formed in the channel lumen.

These favorable computational conclusions encouraged the preparation and membrane characterization of three different hydrophobic CPs (**CP15-17**).[38] Control experiments, with self-quenched LUVs⊃CF, showed a strong detergent effect for **CP17** but leakage was not detected for **CP15** and **CP16** under similar conditions. The standard pH-sensitive LUVs⊃CF assay confirmed the concentration-dependent proton transport for **CP15** and **CP16** and validated the '*in silico*' predicted water strings relay mechanism. Planar BLMs experiments were carried out to quantify the ion transport. The narrow diameter and the partial hydrophobic character of the lumen completely inhibited the ion transport for

hexapeptide **CP15** but ion-borne current was detected for the cyclic octapeptide **CP16**. In symmetric alkali metal ion solutions, **CP16** showed a transport rate in the order of ~10^7 ions s^{-1}, the mean open time was slightly shorter than that of D,L-α-CPs and the overall ion transport efficiency was five times lower. The conductance followed an ohmic behavior for voltages up to 120 mV, suggesting the possible incorporation of two cations in the channel at the same time at higher voltages. The selectivity between cations was minimal and followed the order $Cs^+ > K^+ > Na^+$, with this factor mainly determined by their relative motilities in the bulk solution. However, Na^+ conductance was 30% higher than expected on the basis of the measured conductances and the relative bulk diffusion coefficients.[39] This minimal preference for sodium must be a consequence of the effective size of the conveyed ion and highlights the influence of the dehydration penalty in the transport rate.[39] Transport of Li^+ or Ca^{2+} was not detected in any case – even for **CP16**. The absence of Ca^{2+} transport could be due to the interaction of divalent cations with lipid head groups or to ion trapping within the channel. The low signal/noise ratio of Li^+ events could explain the absence of transport data for this cation. Once again, the observation of 2, 3 or even 4 different nonzero current levels was assigned to nanotubes composed of different CP subunits (Fig. 3b).[21] Computational studies confirmed the stability of the hydrogen-bonded tubular assembly of **CP16** during the simulation time and also showed the rapid entry of both water and cations into the nanotube. The calculated energy profiles for ion transport along the nanotube were lower for α,γ-CPs than for D,L-α-CPs with the same number of Aas. Thus, the ion-solvated passage through the nanotube should be less hampered across the wider but partially hydrophobic inner pore of α,γ-CPs. Simulations also showed a large stabilization of a single Ca^{2+} in the center of the nanotube and no penetration of Cl^- anions in any case, thus explaining the experimental results.

Although SCPN-mediated transport has been widely studied and applied, there is still a great deal of work to be done in this field. Efforts should now focus on lumen functionalization and topological adjustment of the nanotube assembly.[40] The first steps towards the preparation of functionalized γ-Aca have already been achieved with 4-amino-3-hydroxytetrahydrofuran-2-carboxylic acid (γ-Ahf-OH, Fig. 8).[41] This building block was prepared from D-xylose and is equipped with appropriate protecting groups for both solution and solid-phase synthesis. ^{1}H-NMR experiments on the tetrameric model cyclo-[D-Leu-(2*S*,3*R*)-γ-Ahf-D-Tyr(Me)-(1*R*,3*S*)-γ-^{Me}*N*-Acp-] (**CP18**) confirmed the adoption of the required flat conformation of the CP ring with the equatorial hydroxyl substituent pointing inwards in the ensemble. These promising results represent the first step towards the preparation of stable and ordered SCPNs with chemically functionalized lumens. We anticipate that the access to this new class of engineered nanotubes will open a broad range of feasible designs and conceptual devices, such as selectivity filters for artificial ion channels, catalytic pores, receptors or molecule containers.

Supplementary Material

Refer to Web version on PubMed Central for supplementary material.

Acknowledgments

The authors thank Spanish Ministry of Education and Competitivity (MEC) for a Juan de la Cierva Contract (J.M.), and MEC and the ERDF [(CTQ2010-15725, and Consolider Ingenio 2010 (CSD2007-00006)] and the Office of Naval Research (N00014-94-1-0365) and the National Institutes of Health (GM 52190) for financial support.

REFERENCES

1. Stein, WD. Channels, Carriers, and Pumps: An Introduction to Membrane Transport. San Diego, CA: Academic Press; 1990.

2. Hille, B. Ionic Channels of Excitable Membranes. 2nd ed.. Sunderland, MA: Sinauer; 1992.
3. Eisenberg B. Ionic channels in biological membranes: natural nanotubes. Acc. Chem. Res. 1998; 31:117–124.
4. Doyle DA. The Structure of the Potassium Channel: Molecular Basis of K+ Conduction and Selectivity. Science. 1998; 280:69–77. [PubMed: 9525859]
5. de Groot BL, Grubmüller H. Water permeation across biological membranes: mechanism and dynamics of aquaporin-1 and GlpF. Science. 2001; 294:2353–2357. [PubMed: 11743202]
6. Sisson AL, Shah MR, Bhosale S, Matile S. Synthetic ion channels and pores. Chem. Soc. Rev. 2006; 35:1269–1286. [PubMed: 17225888]
7. Chui JKW, Fyles TM. Ionic conductance of synthetic channels: analysis, lessons, and recommendations. Chem. Soc. Rev. 2011; 41:148–175. [PubMed: 21691671]
8. Fyles TM. Synthetic ion channels in bilayer membranes. Chem. Soc. Rev. 2007; 36:335–347. [PubMed: 17264934]
9. Matile S, Vargas Jentzsch A, Montenegro J, Fin A. Recent synthetic transport systems. Chem. Soc. Rev. 2011; 40:2453–2474. [PubMed: 21390363]
10. Bong D, Clark T, Granja J, Ghadiri M. Self-assembling organic nanotubes. Angew. Chem. Int. Ed. 2001; 40:988–1011.
11. Chapman R, Danial M, Koh ML, Jolliffe KA, Perrier S. Design and properties of functional nanotubes from the self-assembly of cyclic peptide templates. Chem. Soc. Rev. 2012; 41:6023–6041. [PubMed: 22875035]
12. Ketchem R, Hu W, Cross T. High-resolution conformation of gramicidin A in a lipid bilayer by solid-state NMR. Science. 1993; 261:1457–1460. [PubMed: 7690158]
13. De Santis P, Morosetti S, Rizzo R. Conformational analysis of regular enantiomeric sequences. Macromolecules. 1974; 7:52–58. [PubMed: 4837982]
14. Ghadiri MR, Granja JR, Milligan RA, McRee DE, Khazanovich N. Self-assembling organic nanotubes based on a cyclic peptide architecture. Nature. 1993; 366:324–327. [PubMed: 8247126]
15. Ghadiri MR, Kobayashi K, Granja JR, Chadha RK, McRee DE. The structural and thermodynamic basis for the formation of self-assembled peptide nanotubes. Angew. Chem. Int. Ed. 1995; 34:93–95.
16. Clark TD, Buriak JM, Kobayashi K, Isler MP, McRee DE, Ghadiri MR. Cylindrical β-sheet peptide assemblies. J. Am. Chem. Soc. 1998; 120:8949–8962.
17. White CJ, Yudin AK. Contemporary strategies for peptide macrocyclization. Nat. Chem. 2011; 3:509–524. [PubMed: 21697871]
18. Ghadiri MR, Granja JR, Buehler LK. Artificial transmembrane ion channels from self-assembling peptide nanotubes. Nature. 1994; 369:301–304. [PubMed: 7514275]
19. Kim HS, Hartgerink JD, Ghadiri MR. Oriented self-assembly of cyclic peptide nanotubes in lipid membranes. J. Am. Chem. Soc. 1998; 120:4417–4424.
20. Bamberg EE, Läuger PP. Temperature-dependent properties of gramicidin A channels. Biochim. Biophys. Acta. 1974; 367:127–133. [PubMed: 4138938]
21. Sanchez-Quesada J, Ghadiri MR. Unpublished results.
22. Hodkin AL, Katz B. The effect of sodium ions on the electrical activity of giant axon of the squid. J. Physiol. 1949; 108:37–77. [PubMed: 18128147]
23. See suporting information
24. Engels M, Bashford D, Ghadiri MR. Structure and dynamics of self-assembling peptide nanotubes and the channel-mediated water organization and self-diffusion.A molecular dynamics study. J. Am. Chem. Soc. 1995; 117:9151–9158.
25. Granja J, Ghadiri M. Channel-mediated transport of glucose across lipid bilayers. J. Am. Chem. Soc. 1994; 116:10785–10786.
26. Sanchez-Quesada J, Kim H, Ghadiri M. A synthetic pore-mediated transmembrane transport of glutamic acid. Angew. Chem. Int. Ed. 2001/B; 40:2503–2506.
27. Sanchez-Quesada J, Isler M, Ghadiri M. Modulating ion channel properties of transmembrane peptide nanotubes through heteromeric supramolecular assemblies. J. Am. Chem. Soc. 2002; 124:10004–10005. [PubMed: 12188661]

28. Motesharei K, Ghadiri MR. Diffusion-limited size-selective ion sensing based on SAM-supported peptide nanotubes. J. Am. Chem. Soc. 1997; 119:11306–11312.

29. Gu LQ, Dalla Serra M, Vincent JB, Vigh G, Cheley S, Braha O, Bayley H. Reversal of charge selectivity in transmembrane protein pores by using noncovalent molecular adapters. Proc. Natl. Acad. Sci. U.S.A. 2000; 97:3959–3964. [PubMed: 10760267]

30. Sanchez-Quesada J, Ghadiri MR, Bayley H, Braha O. Cyclic peptides as molecular adapters for a pore-forming protein. J. Am. Chem. Soc. 2000; 122:11757–11766.

31. Fernandez-Lopez S, Kim HS, Choi EC, Delgado M, Granja JR, Khasanov A, Kraehenbuehl K, Long G, Weinberger DA, Wilcoxen KM, Ghadiri MR. Antibacterial agents based on the cyclic d,l-α-peptide architecture. Nature. 2001; 412:452–455. [PubMed: 11473322]

32. Motiei L, Rahimipour S, Thayer DA, Wong C-H, Ghadiri MR. Antibacterial cyclic D,L-α-glycopeptides. Chem. Commun. 2009:3693–3695.

33. Kienker PK, Degrado WF, Lear JD. A helical-dipole model describes the single-channel current rectification of an uncharged peptide ion channel. Proc. Natl. Acad. Sci. U.S.A. 1994; 91:4859–4863. [PubMed: 7515180]

34. Clark TD, Buehler LK, Ghadiri MR. Self-assembling cyclic β^3 -peptide nanotubes as artificial transmembrane ion channels. J. Am. Chem. Soc. 1998; 120:651–656.

35. Amorín M, Castedo L, Granja JR. New cyclic peptide assemblies with hydrophobic cavities: the structural and thermodynamic basis of a new class of peptide nanotubes. J. Am. Chem. Soc. 2003; 125:2844–2845. [PubMed: 12617629]

36. Brea RJ, Reiriz C, Granja JR. Towards functional bionanomaterials based on self-assembling cyclic peptide nanotubes. Chem. Soc. Rev. 2010; 39:1448–1456. [PubMed: 20419200]

37. Garcia-Fandino R, Granja JR, D'Abramo M, Orozco M. Theoretical characterization of the dynamical behavior and transport properties of a,y-peptide nanotubes in solution. J. Am. Chem. Soc. 2009; 131:15678–15686. [PubMed: 19860480]

38. Garcia-Fandiño R, Amorín M, Castedo L, Granja JR. Transmembrane ion transport by self-assembling α, γ-peptide nanotubes. Chem. Sci. 2012; 3:3280–3285.

39. Eisenman G, Horn R. Ionic selectivity revisited: the role of kinetic and equilibrium processes in ion permeation through channels. J Membr Biol. 1983; 76:197–225. [PubMed: 6100862]

40. Hourani R, Zhang C, van der Weegen R, Ruiz L, Li C, Keten S, Helms BA, Xu T. Processable cyclic peptide nanotubes with tunable interiors. J. Am. Chem. Soc. 2011; 133:15296–15299. [PubMed: 21894889]

41. Reiriz C, Amorín M, García-Fandiño R, Castedo L, Granja JR. α,γ-Cyclic peptide ensembles with a hydroxylated cavity. Org. Biomol. Chem. 2009; 7:4358–4361. [PubMed: 19830283]

Biographies

Javier Montenegro received his PhD (2009) from Professor Susana Lopez at the University of Santiago de Compostela. During this time, he carried out two predoctoral stages in the labs of Prof. Steven Ley (Cambridge) and Prof. Reza Ghadiri (Scripps). In 2009, he moved to the University of Geneva (Switzerland) for his postdoctoral studies with Prof. Stefan Matile. In 2012 he joined the lab of Prof. Juan Granja as a Juan de la Cierva fellow. His research interests are focused in the topological control of supramolecular assemblies for broad applications such as differential sensing, controlled delivery and tubular-templated composites.

M. Reza Ghadiri obtained his PhD in synthetic organic chemistry from the University of Wisconsin, Madison, in 1987, under the guidance of Professor Barry M. Trost. After a two-year postdoctoral fellowship studying enzymology and molecular biology in the laboratory of the late Professor Emil T. Kaiser at the Rockefeller University, he joined the Faculty of Chemistry at the Scripps Research Institute where he is presently Professor of Chemistry and Member of the Skaggs Institute for Chemical Biology. His current research interests include design of peptide therapeutics, bioactive nanostructures, molecular computation,

prebiotic chemistry and adaptive informational biopolymers, programmed enzyme therapeutics, nucleic acid diagnostics, and single-molecule nanopore DNA sequencing.

Prof. Juan R. Granja received the PhD in chemistry from the University of Santiago de Compostela in 1988, under the guidance of Profs. Antonio Mouriño and Luis Castedo, working on the synthesis of vitamin D_2 metabolites. After he moved to Stanford University to carry out postdoctoral studies in the group of Prof. Barry M. Trost. He returned to the University of Santiago as Assistant Professor in 1991. In 1992 he spent six months in the group of, at that time, Assistant Professor M. Reza Ghadiri at The Scripps Research Institute in La Jolla, starting a long and productive scientific collaboration. In 1995 he was promoted to Associate Professor and in 2006 to Full Professor. His research interest is devoted to the synthesis of functional structures focused on peptide nanotubes based on cyclic peptides containing cyclic gamma-amino acids.

The lipid bilayer membranes are Nature's dynamic structural motifs that individualize cells and keep ions, proteins, biopolymers and metabolites confined in the appropriate location. The compartmentalization and isolation of these molecules from the external media facilitate the sophisticated functions and connections between the different biological processes accomplished by living organisms. However, cells require assistance from minimal energy shortcuts for the transport of molecules across membranes so that they can interact with the exterior and regulate their internal environments.

Ion channels and pores stand out from all other possible transport mechanisms due to their high selectivity and efficiency in discriminating and transporting ions or molecules across membrane barriers. Nevertheless, the complexity of these smart "membrane holes" has driven researchers to develop simpler artificial structures with comparable performance to the natural systems. As a broad range of supramolecular interactions have emerged as efficient tools for the rational design and preparation of stable 3D superstructures, these results have stimulated the creativity of chemists to design synthetic mimics of natural active macromolecules and even to develop artificial structures with functions and properties.

In this Account we highlight results from our laboratories on the construction of artificial ion channel models that exploit the self-assembly of conformationally flat cyclic peptides (CPs) into supramolecular nanotubes. Because of the straightforward synthesis of the cyclic peptide monomers and the complete control over the internal diameter and external surface properties of the resulting hollow tubular suprastructure, CPs are the optimal candidates for the fabrication of ion channels. The ion channel activity and selective transport of small molecules by these structures are examples of the great potential that cyclic peptide nanotubes show for the construction of functional artificial transmembrane transporters. Our experience to date suggests that the next steps for achieving conceptual devices with better performance and selectivity will derive from the topological control over cyclic peptide assembly and the functionalization of the lumen.

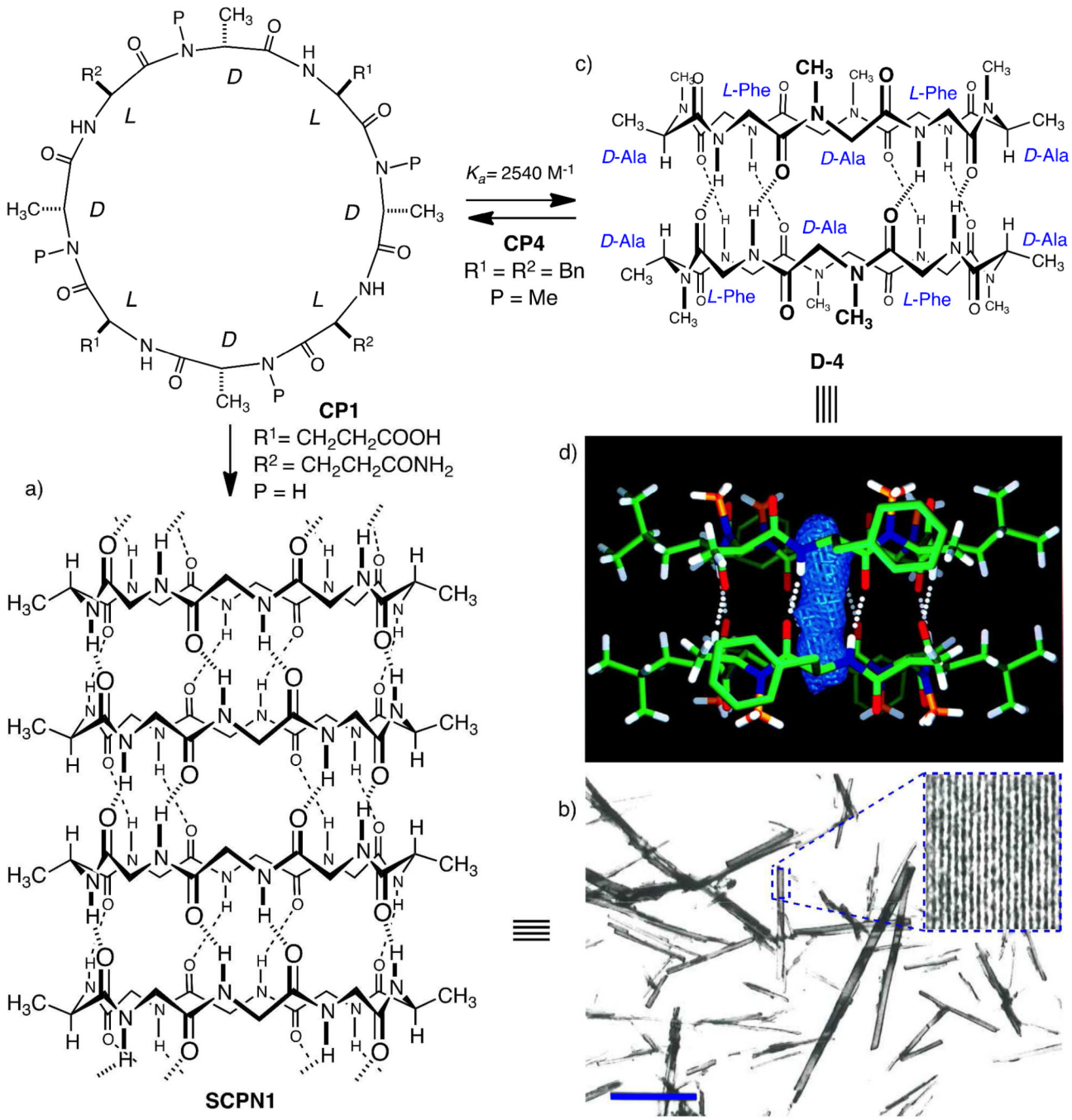

Figure 1.

CP1 and **CP4**. a) Self-assembled nanotube structure of **CP1** (most of the side chains are omitted for clarity). b) Electron microscopy low-magnification image of nanotube suspension adsorbed on a carbon support film (scale bar 1 μm); inset shows low-dose image enhancement of a single crystal and reveals the longitudinal striations that correspond to each nanotube. c) Cylindrical dimer of **CP4**. d) Crystal structure of **D4** emphasizing the internalized water binding sites (blue rod).

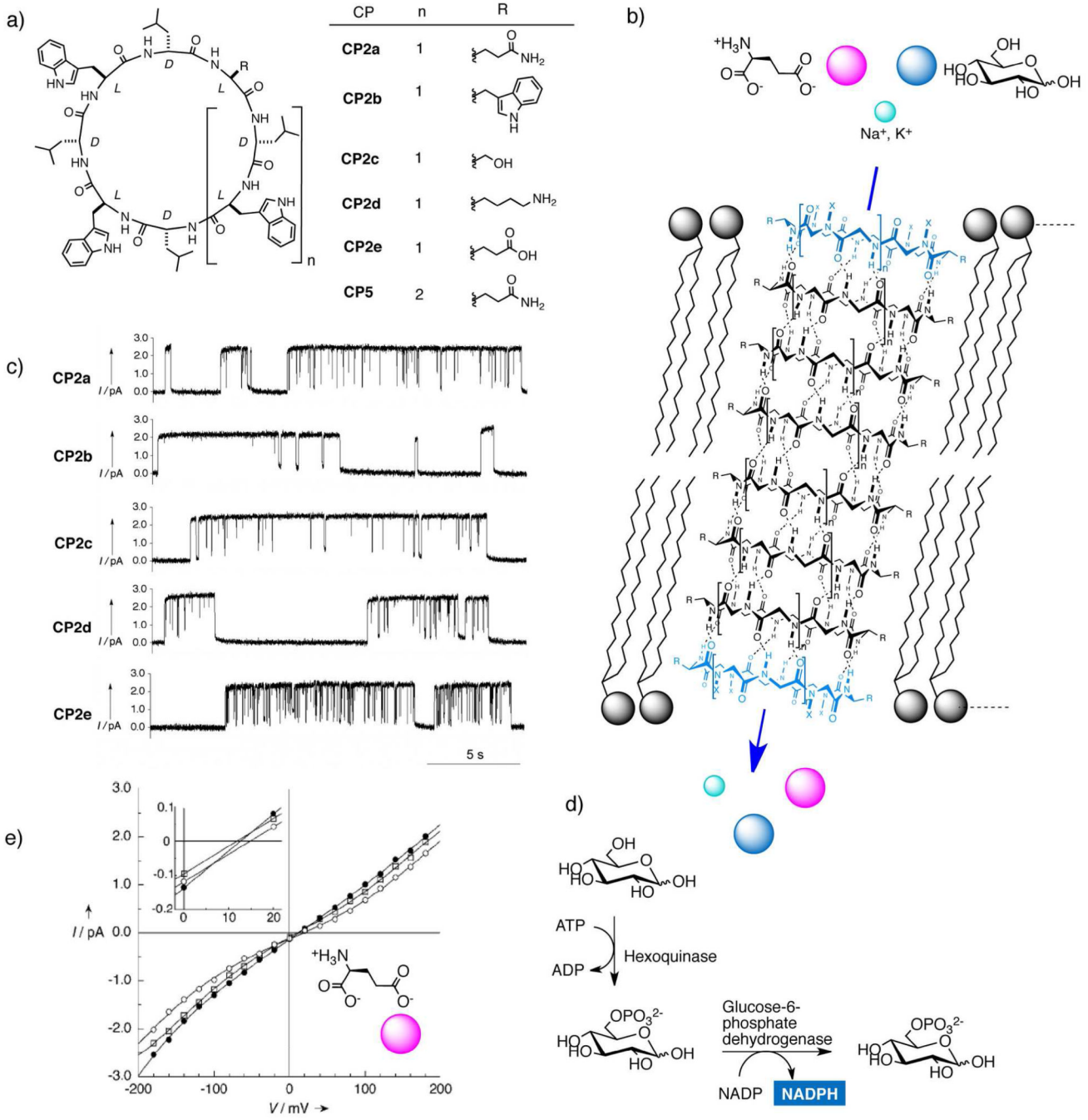

Figure 2.

D,L-α-SCPNs as functional ion channels or pores. a) Structures of **CP2a–e** and **CP5** and b) model of the transmembrane channels in the lipid bilayer (most of the side chains are omitted for clarity), which were able to transport ions (green), glucose (blue) or glutamic acid (red). c) 20-s continuous K^+ (1M KCl) single channel conductance recorded at +100 mV for **CP2 a–e**. d) Enzymatic assay to motorize glucose efflux from liposomes by NADPH detection (**CP5**). e) Current/voltage (*I/V*) plot for gramicidin A (●), **CP2a** (□) and **CP5** (○) in planar BLMs separating NaCl and NaGlu solutions (300 mM). The inset shows the higher

reversal potential required for **CP5**. Figure 2e is reproduced by permission of John Wiley and Sons.

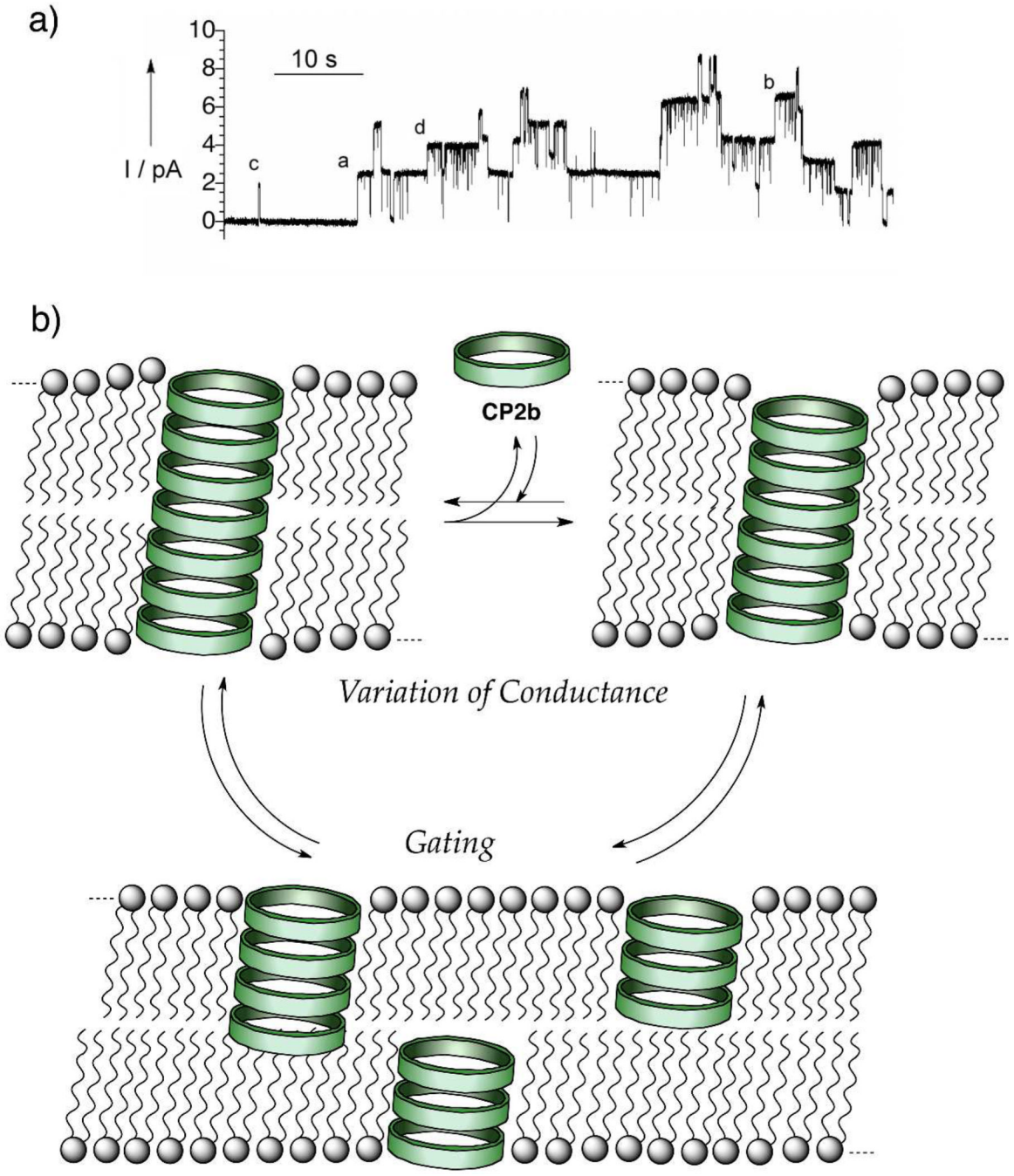

Figure 3.

a) Different conducting states recorded at +100 mV, showing at least four working channels formed by **CP2b** in L-α-lecithin bilayers in 1M KCl. b) Probable mechanisms of gating and of variable conductance events.

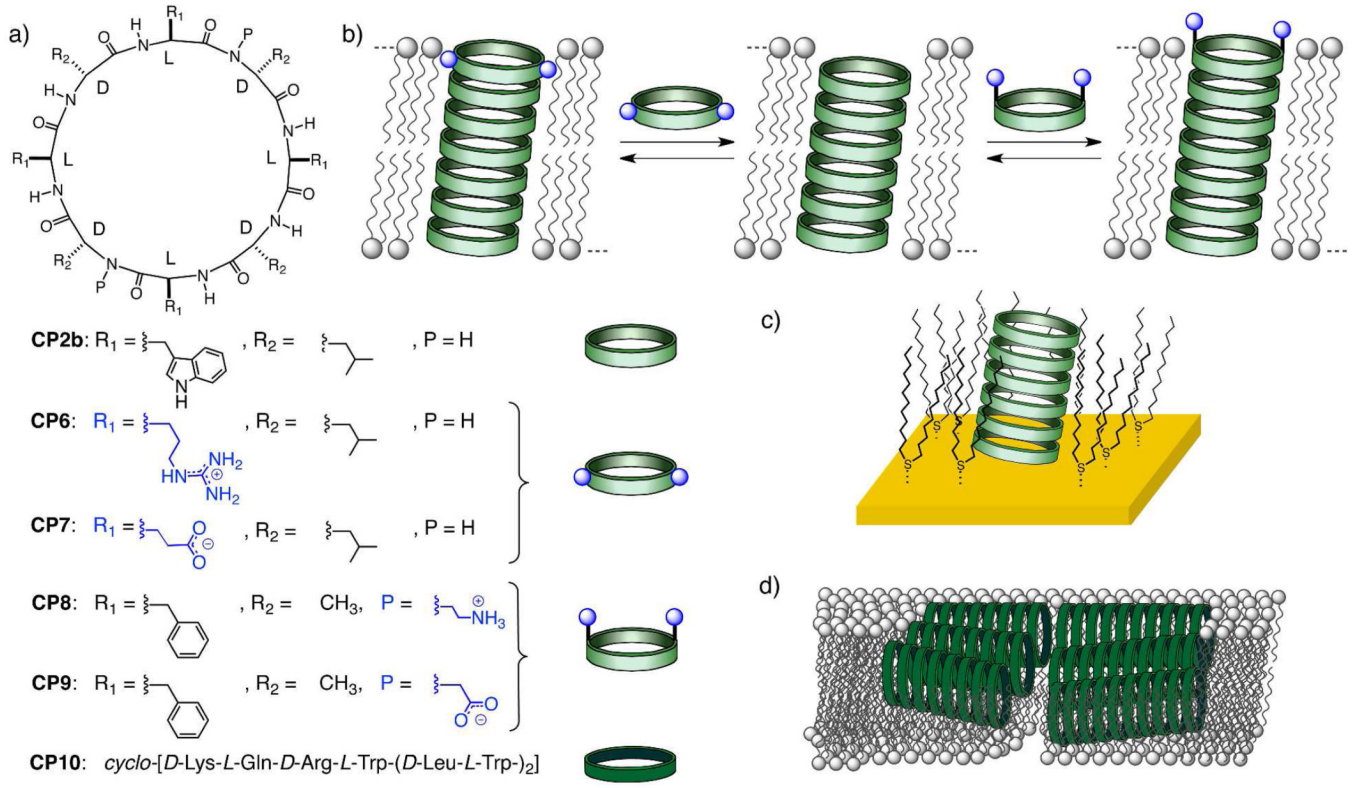

Figure 4.

a) Structures of **CP2b**, **CP6-10**. b) Mode of interaction of the CP caps (**CP69**) with the transporting ensemble of **CP2b** to afford heteromeric transmembrane channels. c) **SCPN2b** embedded in the gold SAMs for the construction of selective ion sensors. d) Proposed model of parallel nanotube orientation for amphiphilic antibacterial D,L-α-cyclic peptides (**CP10**).

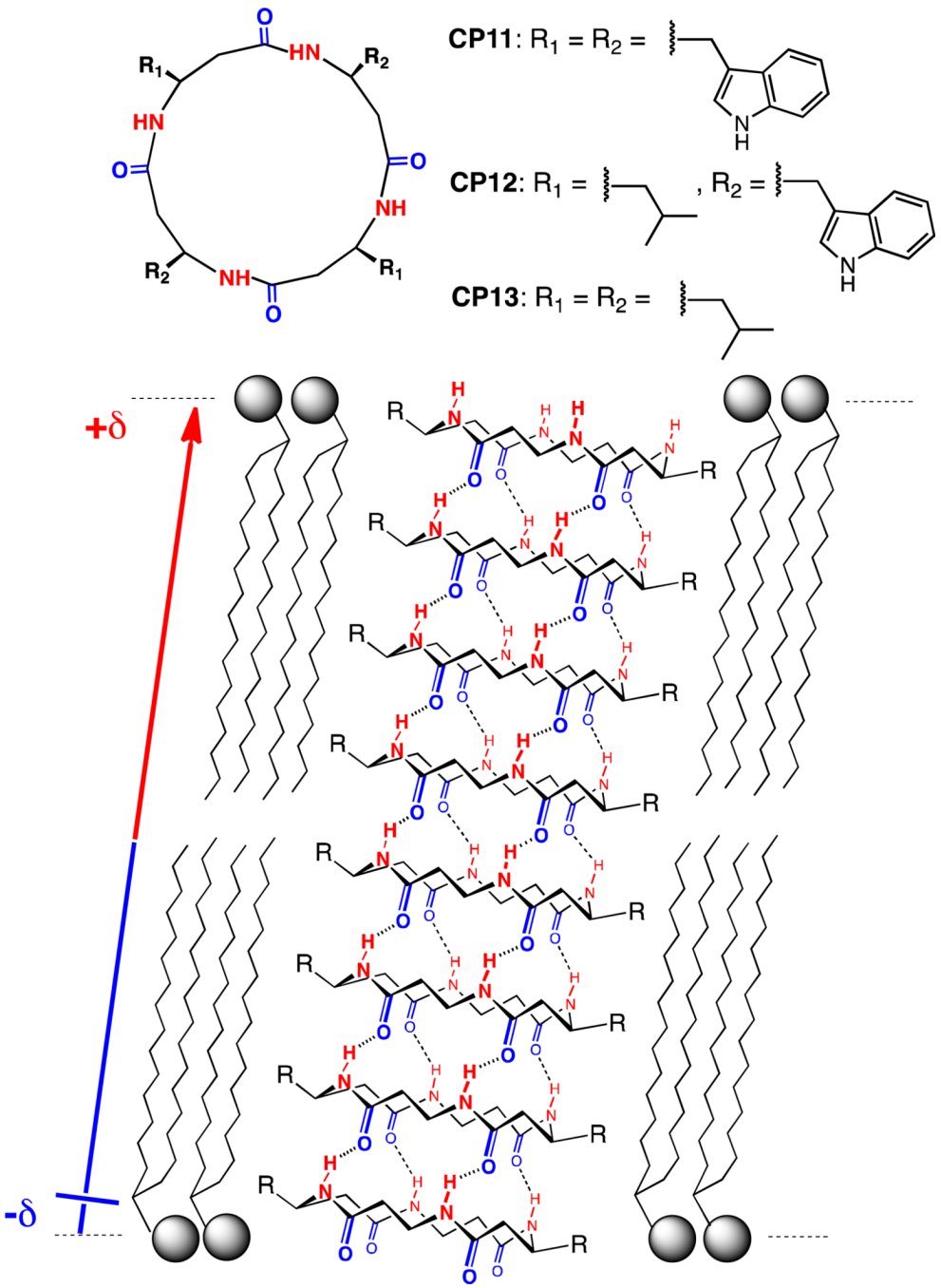

Figure 5.
Structure of β^3-CPs, **CP11-13** and the corresponding membrane β^3-SCPN. The alignment of amide and carbonyl groups generates a net dipole moment.

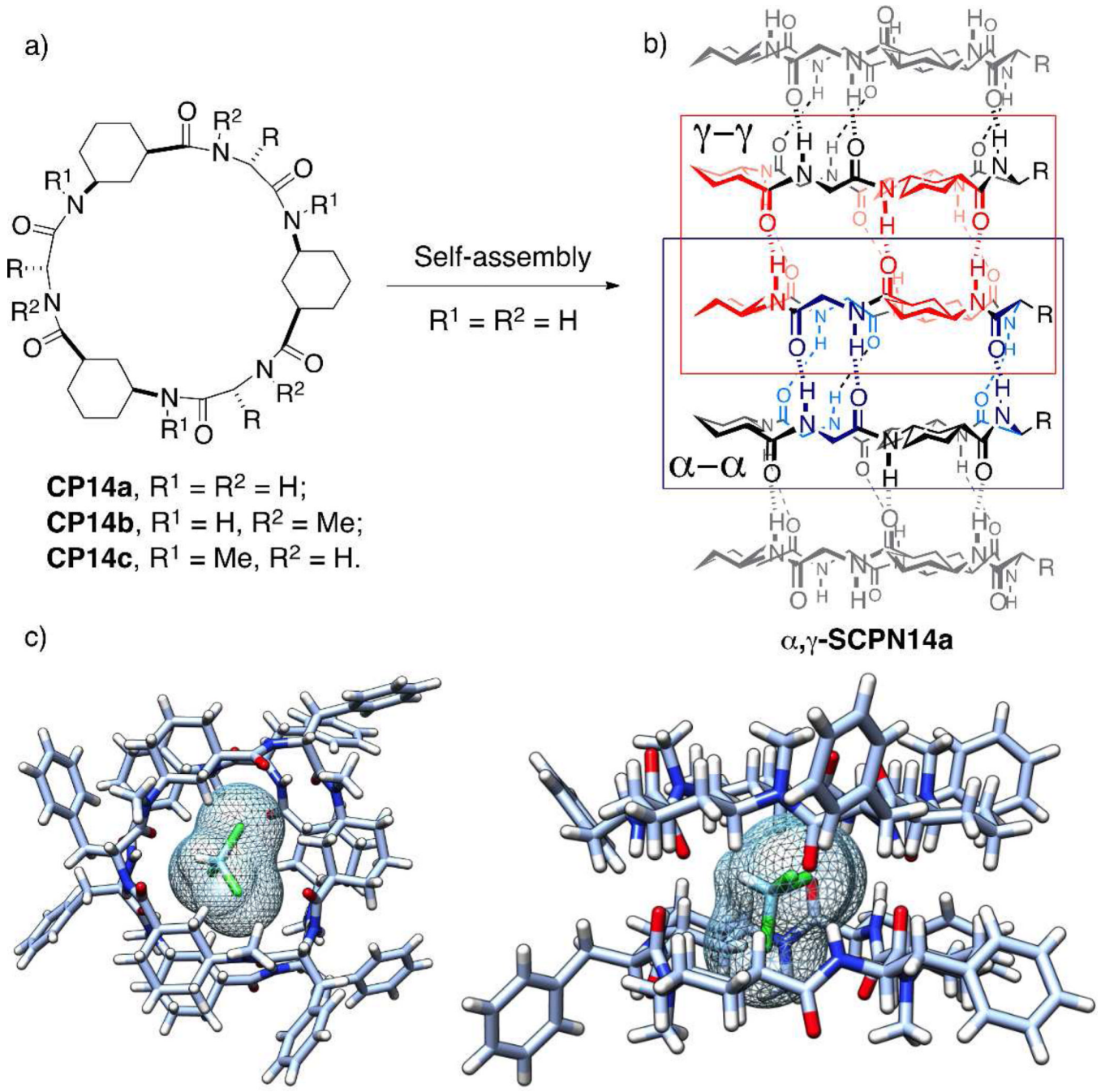

Figure 6.

a) Structure of α,γ-CPs **CP14a**–**c**. b) Different hydrogen-bonding pattern in the tubular arrangement of α,γ-SCPNs. c) Crystal structure of dimeric assembly of **CP14c** (R = Bn), in which one chloroform molecule occupies their cavity: (left) top view; (right) side view.

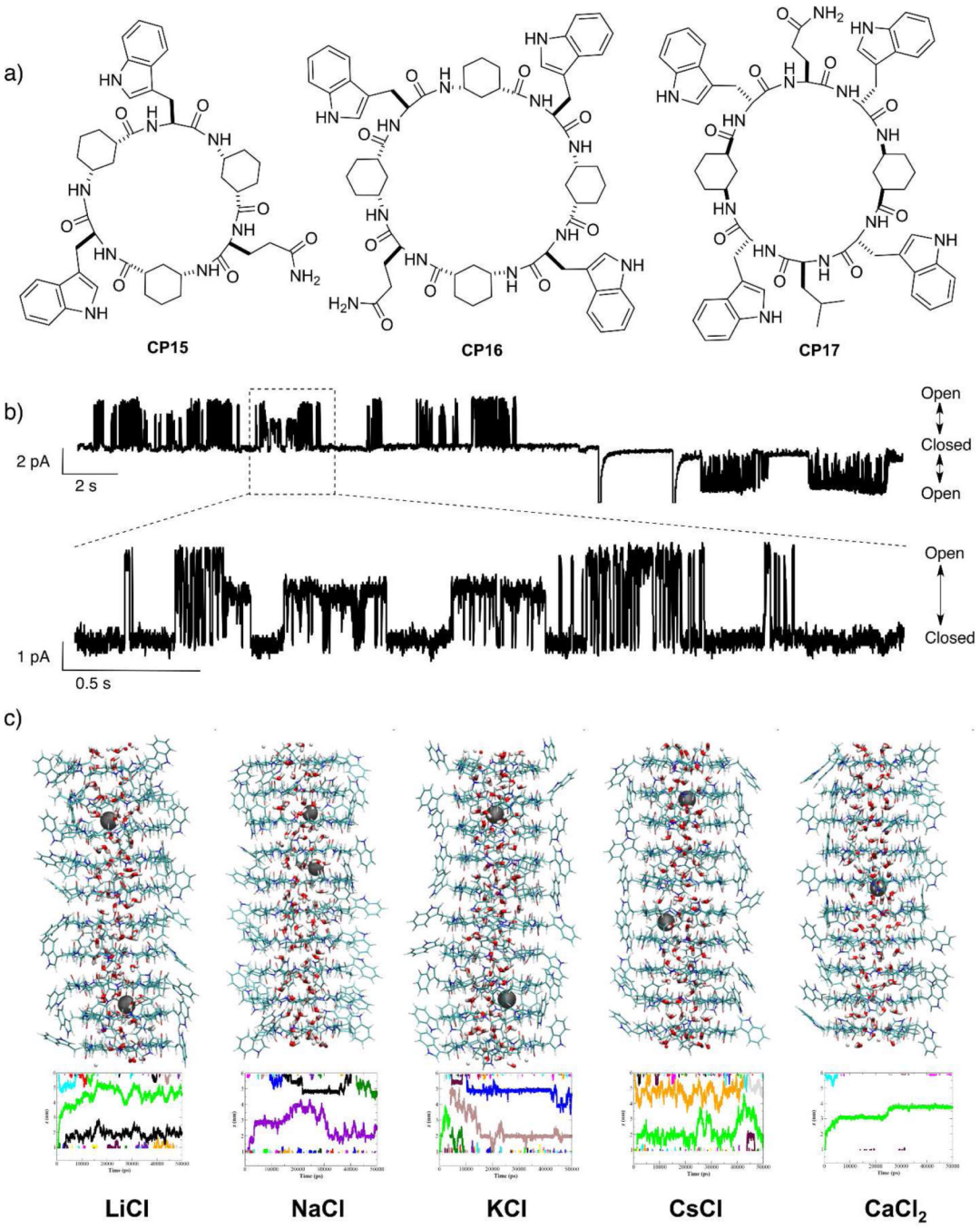

Figure 7.

a) Structure of α,γ-CPs **CP1517**. b) Single-channel recordings of Na^+ current through **CP16** channels (+100 mV and −100 mV) and 3.0 s detail of the trace showing two different current levels (1.8 and 3.1 pA). c) Snapshots of simulated SCPNs in 0.5 M electrolyte solutions after 25 ns of simulation (lipids and external water and ions have been removed for clarity) and Z coordinate for the ions inside the nanotube along the trajectory. [38] – Part of this figure is reproduced by permission of The Royal Society of Chemistry

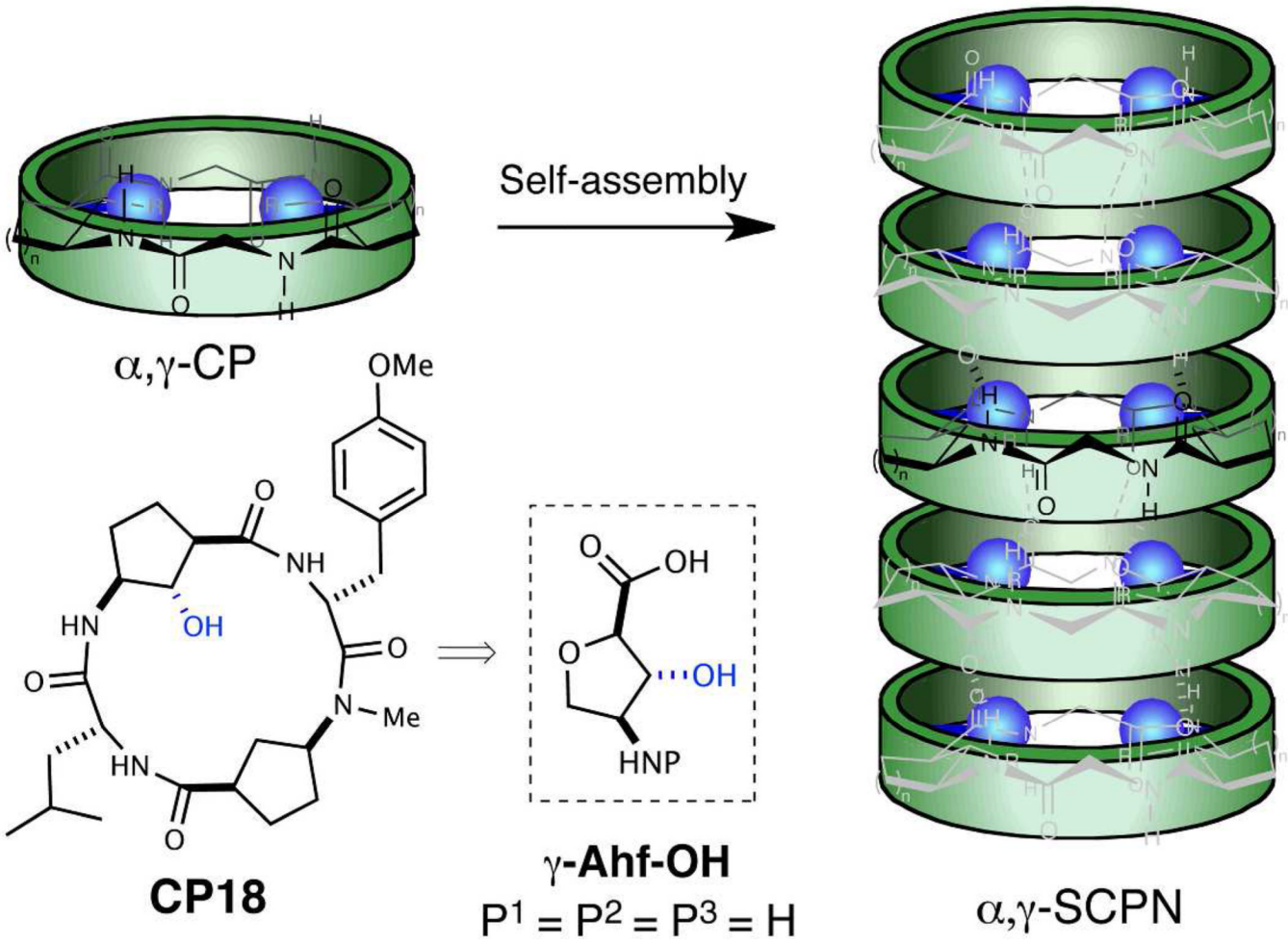

Figure 8.

a) Structure of **CP18** and model for nanotube formation showing the hydroxyl groups (blue color) projected towards the cavity.